Diffusion of chiral molecules and propagation of structural chirality in anisotropic liquids

Mireille Quémener and Tigran Galstian*
Université Laval, Department of Physics, Engineering Physics and Optics Québec, Québec, Canada G1V 0A6

Thomas Marmin, Victoria Laroche, and Yves L. Dory†
Université de Sherbrooke, Département de Biochimie, Sherbrooke, Québec, Canada J1H 5N4
(Received 13 January 2017; published 10 May 2017)

Diffusion in nature is usually considered as a smooth redistribution process. However, it appears that the diffusion of chiral molecules and the propagation of chirality may proceed in quite different ways. Indeed, in the present work, unexpected quantization of the spatial concentration of chiral molecules is discovered in self-aligned molecular liquids. It is shown that the interpenetration of two liquids is forming discrete diffusion barrier walls resulting in steplike concentration distribution of chiral molecules in space. The concentration gradient is at least an order of magnitude stronger from both sides of the barrier wall compared to the gradient between those walls. It is also shown that this microscopic diffusion process may be controlled by macroscopic boundary conditions imposed on the host molecular system. Both of those phenomena are related to the collective long-range orientational "elastic" interactions of molecules of the host. The observed phenomena may radically change our understanding of diffusion of chiral molecules, among others, in biological tissue, which contains many examples of self-aligned molecular liquids. This, in turn, has the potential to revolutionize drug design and delivery techniques.

DOI: 10.1103/PhysRevE.95.052701

I. INTRODUCTION

It is difficult to underestimate the importance of molecular diffusion processes, which are omnipresent in nature. Particularly important is the understanding of mechanisms affecting the diffusion of chiral molecules since many biologically important molecules and the majority of drugs are chiral [1]. In fact, both the creation and propagation of chirality in nature were and still are a matter of passionate debate since the pioneering works of Louis Pasteur [2]. At the same time, the biological tissue is rich with self-assembled and oriented molecular complexes, such as cell membrane and myelin [3], mucus [4], synovial fluid [5], and biofilm [6,7]. Such angularly correlated molecular complexes are in a liquid state, but their orientation exhibits a unique (for a liquid) property: the "elasticity"; i.e., it may be deformed by a stress and it recovers the original orientation after the stress is released. As we can see below, this elasticity may dramatically affect the diffusion processes of chiral molecules and their medicinal impact. Indeed, important changes of medical functionalities were recently reported that are related to the molecular aggregation in the brain [8]. A hypothesis was suggested, followed by its preliminary experimental exploration [9], that self-aligned molecular complexes, abundantly present in the brain, might reduce the diffusion of chiral molecules causing their aggregation. This hypothesis was speculating that, in addition to well-known factors affecting the molecular diffusion, the large-scale angular correlation of molecular interactions of the host media might be at the origin of such decrease of diffusion. Unfortunately, that hypothesis was not supported by direct experimental evidence because of the unavailability of easily traceable (e.g., by fluorescence) chiral molecules. It is worth mentioning that there have been other attempts to study the diffusion of chiral (nonfluorescent) molecules in a self-aligned liquid crystal (LC) matrix by using nondirect optical [10,11] or nuclear magnetic resonance [12] techniques. However, the diffusion barrier problems and the role of the orientational elasticity (particularly of boundary conditions) on chiral diffusion processes have not been addressed.

In the present work we have synthesized a chiral fluorescent molecule (CFM) to study the above-mentioned diffusion processes. The use of this molecule enabled the direct quantification of chiral molecular diffusion in a self-aligned liquid matrix. This allowed us to validate the original hypothesis (the role of the macroscopic elasticity in the microscopic diffusion process), and, in addition, to discover an unexpected phenomenon of molecular concentration quantization (abrupt steplike changes of chiral molecular concentration in the liquid host) due to diffusion barriers that are naturally formed by molecular orientation defects in the host. This paper starts by describing the material system (the guest CFM and the host LC matrix) and the structure of the chamber used in our experiments. Then we describe the experimental methodology (setups and processes) used to quantify the diffusion of guest molecules. We then describe and analyze the obtained results, followed by conclusions.

II. MATERIALS AND CHAMBERS

Guest molecule. Although chiral drugs are numerous, fluorescent chiral therapeutics are scarce. One such molecule, doxorubicin, a very potent anticancer agent belonging to the anthracycline family, is conveniently used as a theranostic agent, owing to its inherent fluorescence [13]. However, the high toxicity of this natural chiral compound is a major hurdle to its study in media mimicking biological self-assembled molecular complexes. Therefore, we designed an alternative molecule, 1, that could meet all the requirements in terms of

*tigran.galstian@phy.ulaval.ca
†yves.dory@usherbrooke.ca

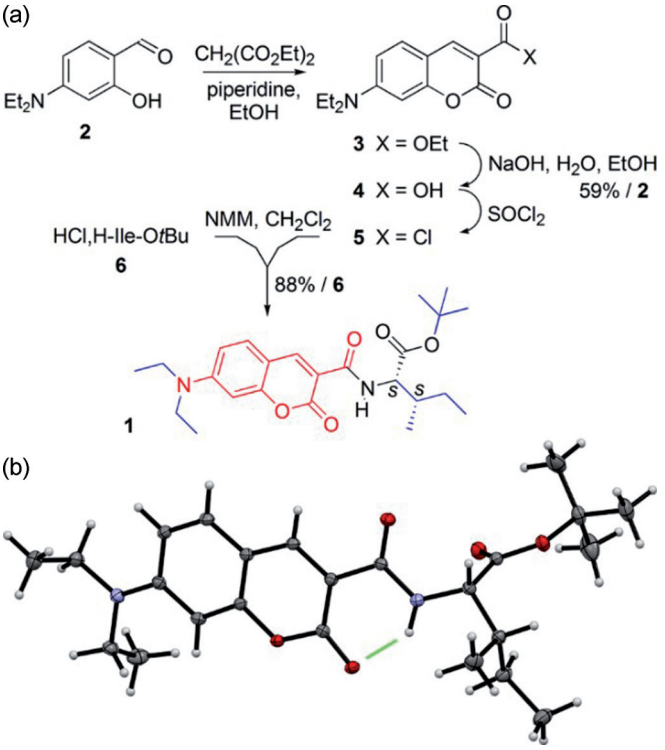

FIG. 1. Identity of chiral fluorophore 1. (a) Synthesis of 1 (blue and red parts indicate lipophilic and fluorogenic regions, respectively). (b) X-ray crystal structure of 1 (green dash indicates intramolecular H bond). The structure was deposited at the Cambridge Crystallographic Data Centre (CCDC No. 1518911).

chirality, fluorescence, and miscibility (Fig. 1). It is basically a chiral amino acid, isoleucine (Ile), coupled to a fluorescent coumarin [14,15] through an amide linkage [16,17]; the C terminus is protected as a *t*-butyl ester. Compound 1 is particularly soluble into the lipophilic LC matrix, due to its lipophilic Ile *i*-butyl, *t*-butyl, and diethylaniline groups. Moreover, 1 is amenable to large-scale synthesis [18]. It was prepared via a four-step sequence starting from 4-diethylamino-salicaldehyde 2. Diethyl malonate underwent a Knoevenagel condensation with 2 to produce the coumarin ester 3, which was not isolated [17]. Rather, it was directly hydrolyzed to the coumarin acid 4, that was easily purified by crystallization [14]. Subsequent treatment of the acid 4 with thionyl chloride yielded the corresponding acid chloride 5, which was immediately coupled with the Ile amine derivative 6 [17], without further purification and in good yield (88% from 6). The resulting product 1 was then crystallized and its structure was confirmed by crystallography. On the whole, the structure is rather rigid because of an intramolecular H bond between the amide NH (donor) and the coumarin lactone CO (acceptor). Consequently, the conformation of the molecule is partially locked and the amide bond is probably unable to participate in intermolecular weak interaction apart from nondirectional van der Waals.

The design of molecule 1 is very relevant to all drugs. Compound 1 is not a drug itself, but it complies with all the requirements listed by Lipinski *et al.* [19] and Veber *et al.* [20] for best drug candidates (Table I). Its molecular weight is below 500 g mol^{-1} and its calculated hydrophobicity is below 5. It contains fewer than five H-bond donors and fewer than ten H-bond acceptors. Having a polar surface area of 85 Å^2 [21], 1 would be a very good drug candidate in general and it could even target the central nervous system. Moreover, the number of rotatable bonds is under 12 as requested by Veber and co-workers.

The fluorescence spectrum of the above-mentioned molecule is centered at 460 nm with a full width (measured at half maximum) of approximately 50 nm.

Host media. The single molecular composition liquid 4-cyano-4′-pentylbiphenyl (with the chemical formula $C_{18}H_{19}N$, commonly named as 5CB) was used as host (from Sigma-Aldrich, without further modification). This liquid is in self-aligned LC phase in the temperature range between 18 °C and 35 °C. All our experiments have been conducted in this phase, at room temperature (20.1 °C ± 0.1 °C).

Chambers. Optical chambers were fabricated in the form of sandwiches with two glass substrates that were kept at the distance of $d = 9.8\,\mu\text{m} \pm 0.7\,\mu\text{m}$ by using glass spacers (from Duke Standards) mixed with UV curable adhesive (Norland Optical Adhesive 65) that was dispensed in the periphery of the chamber to form its walls. Those chamber walls contained two holes (positioned at opposite corners of the sandwich) to be used to fill (by capillarity) the sandwich by the desired liquid (see hereafter). Special care was paid to obtain uniform thickness of the sandwich to avoid the appearance of local bends or wedges. Inner surfaces of substrates were coated (by standard spin coating technique) by a 60-nm-thick polyimide layer (PI-150, from Nissan) to ensure the alignment of LC molecules in the plane of substrates. In 50% of the cases, we have mechanically rubbed (with a tissue) the PI-150 layer in one direction (say $+y$) for one of the substrates of the sandwich. Then the PI-150 of the opposite substrate (of the

TABLE I. Correspondence of the molecule 1 to requirements for drugs.

	Properties	Optimal values	1
Lipinski *et al.* [19]	Molecular weight	<500 g mol^{-1}	430
	c log *P*	<5	∼4
	Number of H-bond donors	<5	1
	Number of H-bond acceptors	<10	4
Veber *et al.* [20]	Polar surface area	<140 Å^2 (general) <90 Å^2 (CNS)	85 Å^2
	Number of rotatable bonds	<12	6

same chamber) was rubbed in the opposite direction $(-y)$. Then those two substrates were assembled with "antiparallel" rubbing directions. In this way, we "macroscopically" impose an alignment direction (along the y axis [22]) for the average orientation of LC molecules (called "director," representing the local anisotropy axis of the LC). We shall further define those sandwiches as having "strong" boundary conditions (corresponding to planar alignment with well-defined direction of LC molecules). In the remaining 50% of chambers, there was no rubbing and thus the molecules of the LC were relatively free to rotate in the plane of substrates, while still remaining in the plane. We shall further define those sandwiches as having "weak" boundary conditions.

Procedure. Approximately three-fourths of the sandwich was filled (using capillarity) by the pure 5CB host from one of the wall holes of the sandwich. A saturated mixture of the CFM and 5CB was prepared separately with the concentration of CFM $= 0.012$ g/ml. This mixture was inserted (also using the capillarity effect) into the sandwich (approximately one-fourth of the volume) from the opposite wall hole of the sandwich.

The capillary propagation of both liquids and their physical contact formed the interface (hereafter called "contact" interface) between those two liquids. The neighborhood of this interface was studied using a Zeiss Axiovert microscope with a $10\times$ objective and the corresponding images were recorded using an AmScope Mu300 camera. The lateral resolution of our system at the fluorescence wavelength was approximately $2\ \mu$m.

III. EXPERIMENTAL RESULTS

Microscopic images of the contact interface between two liquids (with and without the CFM) were recorded at different times (after the contact was formed). We have discovered that the diffusion process in our liquid has generated a macroscopic network of discrete "lines" (mainly parallel to the contact interface; see hereafter) that were clearly visible even when the chamber was illuminated by the white light source of the microscope without using polarizers. The sandwich was also placed between crossed polarizer and analyzer (standard polarimetric setup) and illuminated by the same white light source (the CFM was not excited in those experiments). Figure 2 shows an example of six discrete zones (or bands) that appeared (along with the diffusion process) between the above-mentioned network of lines. As we can see, different bands have different colorations, separated by "vertical" lines that are parallel to the contact interface [9]. Figure 2 also shows one "horizontal" line in the upper part of the second band (from the left).

However, many such lines were formed in other bands [particularly in zones with high concentration of CFM; see, e.g., two such lines in the inset of the Fig. 2(a), on the top right].

The same contact interface was also studied using a quasimonochromatic light (by adding a green pass-band filter to the same polarimetric setup). As it can be seen from Fig. 2(b), the addition of that filter eliminates various band colors (as expected) and generates different intensities of transmitted green light. This shows that we are observing different degrees of light polarization modulation (ellipticity

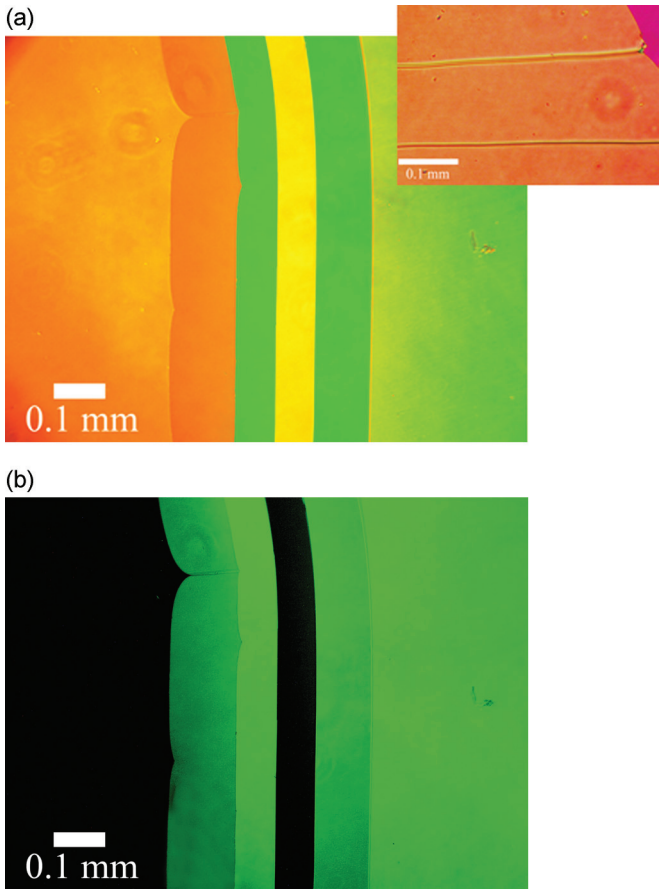

FIG. 2. The microscope photography of the contact interface between two liquids (and its neighborhood) in the ground state of the CFM. The extreme left band in the image represents the zone having higher concentration of the CFM. (a) The sandwich is placed between crossed polarizers and a white light source is used to illuminate the sandwich. Inset (top right): example of two parallel horizontal lines. (b) A pass-band interferential filter is added to the setup (the sandwich is still placed between crossed polarizers).

and rotation of the polarization plane) from band to band. For example, the output (from the chamber) light's polarization is almost linear and perpendicular to the transmission axis of the analyzer in zones 1 and 4 (from the left), while it is almost parallel to the analyzer's transmission axis in zones 3 and 6 (from the left).

While those results clearly show that discrete zones are naturally formed in the host liquid as a result of the diffusion of CFM, the role of its concentration distribution in space may be better understood by using the fluorescence of the CFM. We have thus studied the spatial distribution of the intensity of the fluorescence of the CFM in the neighborhood of the contact interface. In this experiment, the CFM was excited by using an EXFO X-cite 120 light source with Chroma filters (to select the optimal CFM excitation wavelengths, around 385 nm) that was incorporated into the microscope (no polarizers were used here). Figure 3(a) shows an example of typical results obtained. The intensity profile is continuously changing within each zone with a gradient that is perpendicular to the contact interface in both (weak and strong alignment) cases. However, it is very surprising to see abrupt changes of fluorescence intensity.

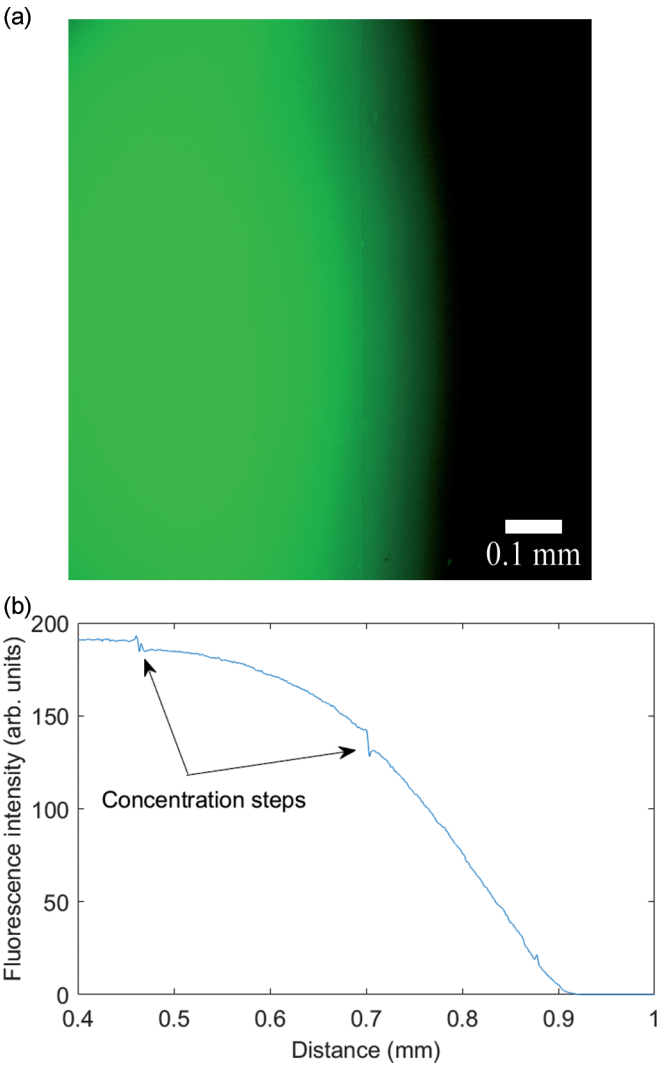

FIG. 3. Spatial distribution of the intensity of the fluorescence of the excited CFM in the neighborhood of the interface between two liquids (the CFM is excited here and there are no polarizers). (a) The image of spatial distribution of fluorescence. (b) The intensity distribution of the fluorescence in the direction perpendicular to the contact interface. Images were processed by using IMAGEJ software and the intensity was determined by MATLAB.

Their positions coincide with the positions of vertical lines (parallel to the contact interface) that were observed in Fig. 2. Figure 3(b) represents the intensity histogram in the direction perpendicular to the contact interface [obtained from Fig. 3(a)]. One can clearly distinguish "discrete" steps of fluorescence intensity.

Obviously, we must insure that the intensity of the fluorescence adequately represents the concentration of the CFM. For this purpose, multiple sandwiches (without the PI-150 layer and without any surface treatment) were fabricated with different concentrations of the CFM (the concentration of CFM was uniform within each sandwich). Their fluorescence intensities (versus the CFM concentration) were measured in the same excitation conditions. As one can see from Fig. 4, the fluorescence intensity depends linearly upon the concentration of the CFM. This confirms that the intensity steps observed (in Fig. 3) indeed represent discrete levels of concentration of the CFM.

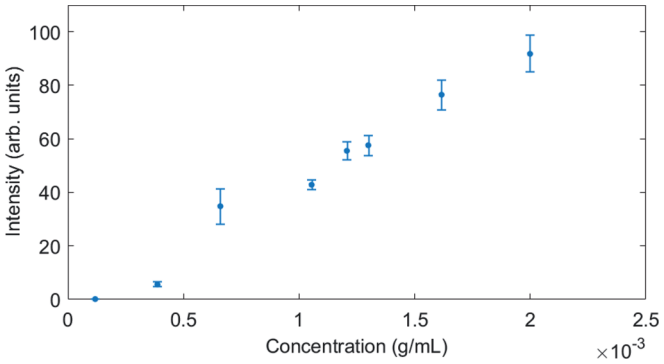

FIG. 4. Intensity of the fluorescence versus the concentration of the chiral fluorophore.

All the above-mentioned experiments were repeated for two types of chambers with strong and weak boundary conditions. The formation of discrete zones was observed in both cases. However, the dynamics of the formation and evolution of those zones was different for those two cases (see below).

IV. DISCUSSION

To understand the origin of discrete structures with steplike concentration distribution in space, generated by the diffusion of molecules in a liquid, we need to use some fundamental concepts governing chiral interactions in self-oriented liquids. Indeed, it is well known that the introduction of chiral molecules (in our case, the CFM) into uniaxial LCs (such as the 5CB) may force the LC molecules to self-organize in the form of a helix [23,24]. In the particular case of planar boundary conditions [22] (where LC molecules are forced to stay in the plane of substrates of the sandwich, as in the present work), the local director of the LC is rotating from one molecular layer to the next layer and the axis of this helix is perpendicular to chamber substrates [23]. The pitch P_0 of the helix (the distance at which LC molecules perform a 360° rotation) is inversely proportional to the local concentration $C(x,t)$ of chiral molecules and directly proportional to their rotation power $P_0 = \gamma C^{-1}$ [23,24]. Often those materials are locally reciprocal and thus the physical properties of the medium are repeated at every 180° rotation. Thus in our future discussions we shall consider the pitch of the material as $P = P_0/2$. It is also well known that, in the case of preferential (strong) boundary conditions, the energetically allowed rotations must be quantized to multiples of 180° since the orientation of molecules on the top and bottom substrates must be aligned in the rubbing direction $\pm y$ [23]. This is the reason why in sandwiches with tilted substrates (wedge chambers), different discrete zones may naturally be formed (when filled with a compositionally uniform chiral LC), with LC molecules performing the same number k of rotations (within the same zone) between two substrates of the chamber ($d = kP_k$, for the thickness d of the LC cell, k being an integer and P_k being the local pitch), and this number k changes from zone to zone. Since two neighboring zones contain different numbers of helices, the molecular orientation cannot be smoothly

transformed from one zone to the next one. Thus they must be separated by "walls" of abrupt changes of molecular orientation in space (so-called "disclinations"), which look like "lines" in the microscope. Such spatial quantization of molecular orientation, separated by orientation defect walls (both parallel and perpendicular to zone frontiers), has already been observed for *uniform* chiral LC materials in *wedge*-shaped sandwiches [23]. As we have already mentioned, similar discrete zones (separated by defect walls) have been also observed in cells with nonuniform concentrations [10,11]. More detailed description of those truly fascinating defect walls may be found, for example, in Ref. [25].

We think that the observed (in our experiment) discrete colored zones (bands) are areas where the LC molecules perform the same number of rotations (within the same zone) between two *parallel* substrates of the chamber, similar to those described in [10]. With the increase of the CFMs' local concentration $C(x,t)$, the LC host tends to adopt a twisted molecular state with shorter pitch $P(x,t)$. However, the optimal rotation rate being different from point to point (since the value of C is different), the material system must adjust the value of $P(x,t)$ to minimize its energy. As a result, large bands are formed where the pitch of the helix is changing very slightly (within the band) and those areas are separated by narrow zones where the orientation of molecules changes very abruptly to accommodate two neighboring bands with one cycle of 180° rotation of difference. The vertical lines observed in our experiment (parallel to the contact interface), that delimit those bands, are thus walls of abrupt changes of molecular orientation between two (differently colored) bands having different numbers of quantized molecular rotations.

According to the theory of de Vries [26] (see also [23]) such twisted structures will rotate the polarization of input light (with wavelength λ) at a specific angle ψ:

$$\psi = d\frac{q_0}{32}\left(\frac{n_e^2 - n_0^2}{n_e^2 + n_0^2}\right)^2 \frac{1}{\lambda'^2(1-\lambda'^2)}, \tag{1}$$

where n_e and n_0 are local extraordinary and ordinary refractive indices of the LC and $\lambda' = \lambda/P_0 = q_0/k_0$ (with q_0 and k_0 being the wave vectors of the helical structure and of the incident light, respectively). While this formula was derived for small optical birefringence values $\Delta n \equiv n_\parallel - n_\perp$ (typically chiral LCs have $\Delta n \approx 0.02$, which is certainly not the case of our host material with $\Delta n_{5\mathrm{CB}} \approx 1.719 - 1.528 \approx 0.2$, measured at room temperature at $\lambda = 632.8\,\mathrm{nm}$ [27]), we can still use it for the qualitative understanding of the origins of band coloration in our case. As we can see from de Vries's equation, for given material properties, the polarization rotation angle ψ is defined by the ratio of λ and $P(x,t)$ as well as by the dispersion of the host material $n_{e,0}(\lambda)$. Thus two neighboring bands with different pitches P should generate different degrees of polarization modulation for different wavelengths. Consequently, we obtain different extinction ratios and resulting light colors for different bands after passing through the analyzer.

The diffusion process taking place in our system is a rather complex phenomenon where the anisotropic processes are conjugated with elastic forces. A theoretical treatment of non-Fickian diffusion that includes the interaction of chirality and anisotropy in gas diffusion (in a cell with one air-open interface) was given in Ref. [28].

In the present work, the situation is more complex and in our further analyses, we shall use a simplified approach to demonstrate the role of boundary conditions in the observed diffusion processes. Thus the width of each colored band will define the critical CFM concentration values (say, C_i and C_{i+1}, at the frontiers of "i" and "$i+1$" bands) at which one additional rotation of 180° is energetically justified; i.e., the additional twisting energy (due to the additional concentration of CFM) is enough to generate an additional 180° orientation twist (with slightly adjusted pitch of the helix to satisfy the orientation requirement in the case of strong boundary condition) and an additional disclination wall. As it can be seen hereafter, the "price" for this pitch adjustment (as well as the difference in the disclination structures) will noticeably affect the diffusion process. Following this model (suggesting that the distances between neighboring vertical lines define the "threshold" concentration difference $\Delta C_{\mathrm{th}} = C_i - C_{i+1}$) and considering the spatial profile (along the direction x, perpendicular to the contact interface) of CFM concentration (retrieved by using Figs. 3 and 4), recorded at different times t, we have found the effective diffusion coefficients of the CFM by using a simplified model described by the equation [29]

$$C(x,t) = \frac{1}{2}C_0\,\mathrm{erfc}\left(\frac{x}{2\sqrt{Dt}}\right). \tag{2}$$

This model suggests that the concentration of CFMs at $x = 0$ (contact interface) is constant; $C(0,t) = C_0 = \mathrm{const}$. We might also use an alternative fitting formula $[C(x,t) = \frac{M}{\sqrt{\pi Dt}}\exp(\frac{-x^2}{4Dt})]$ that takes into account the dynamic changes of $C(0,t)$. However, we have discovered that Eq. (2) describes better our experimental observations [$C(0,t) \approx \mathrm{const}$], and, in addition, the obtained results in both cases are of the same order of magnitude, while the fitting error is much smaller in the case of using Eq. (2). Thus the diffusion was modeled with the help of this equation. For each given time t_0, the spatial profile of the fluorescence intensity along the x axis [proportional to the concentration profile $C(x,t_0)$] was recorded and the numerical fit was done to obtain the effective value of diffusion coefficient $D(t_0)$. The obtained results are presented in Fig. 5.

The fitting procedure was repeated for both types of sandwiches (with strong and weak boundary conditions). Let us remind the reader that, in contrast to the case of strong boundary conditions, there is no strong requirement for the molecular orientation of LC to be parallel to a specific direction at the surfaces of two glass substrates since there is no rubbing here [22]. Thus there is no need for additional adjustment of the pitch. Consequently, the LC is subjected to fewer elastic constraints to "accommodate" the diffusion of CFM and thus the diffusion process should be more effective (see hereafter). However, it is worth noting that the formation of defect walls must happen in all cases, while with different disclination structures [25].

The obtained results (dots) and the polynomial fit (solid line) are presented in the Fig. 5 in the case of weak boundary conditions (the fit formula used was $D = 3.524 \times 10^{-11}x^{-0.461}$, standard error: $1 \times 10^{-12}\,\mathrm{m^2/s}$; determination coefficient, $R^2 = 1$; confidence interval: 95%). The diffusion

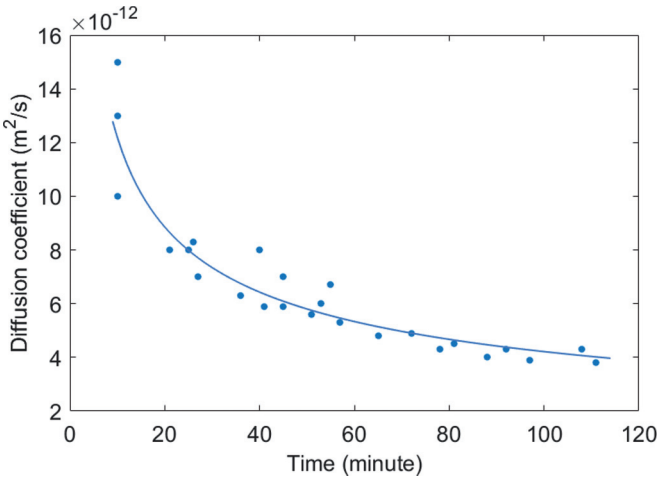

FIG. 5. Effective diffusion coefficient in the case of weak boundary conditions (no rubbing).

coefficient D_w obtained for the weak boundary conditions initially (within the first 10 min after the contact interface was formed) was relatively high, $D_w \approx 12.19 \times 10^{-12}\,\mathrm{m}^2/\mathrm{s}$, and then decreased with time (after 120 min) down to $D_w \approx 3.874 \times 10^{-12}\,\mathrm{m}^2/\mathrm{s}$ (with a time averaged value of $8.03 \times 10^{-12}\,\mathrm{m}^2/\mathrm{s}$, which is of the same order of magnitude as the diffusion coefficients of perylene diimide molecules in 5CB, $D_{\parallel} \approx 8.47 \times 10^{-12}\,\mathrm{m}^2/\mathrm{s}$ and $D_{\perp} \approx 5.75 \times 10^{-12}\,\mathrm{m}^2/\mathrm{s}$, measured by using the NMR technique, respectively, along and perpendicular to the LC's director, [30]).

The case of strong boundary condition is very similar, but with a downshifted curve (demonstrating thus lower diffusion coefficients). Indeed, the similar processing of data for this case (fit formula $D = 2.34 \times 10^{-11} x^{-0.415}$, standard error $0.8 \times 10^{-12}\,\mathrm{m}^2/\mathrm{s}$, determination coefficient $R^2 = 1$, and confidence interval 95%) provides initial (within the first 10 min after the contact interface was formed) diffusion coefficient D_s that is noticeably smaller, $D_s \approx 8.99 \times 10^{-12}\,\mathrm{m}^2/\mathrm{s}$, and then it further decreases (after 120 min) down to $D_s \approx 3.204 \times 10^{-12}\,\mathrm{m}^2/\mathrm{s}$ (with a time averaged value of $6.10 \times 10^{-12}\,\mathrm{m}^2/\mathrm{s}$).

Thus the diffusion of the same CFM in the same LC host at the same temperature and the same concentration gradient values is noticeably stronger (by 36%) in the case of weak boundary conditions, the discrimination factor $R \equiv D_w/D_s$ starting at 1.36 (at $t = 10$ min), and decreasing with time down to 1.21 after 120 min (25% of difference in average). It is truly remarkable that a *microscopic* phenomenon (molecular diffusion) can be controlled by using such a simple *macroscopic* method (rubbing the inner surfaces of the chamber) due to the collective molecular orientational interactions of the host.

However, it is even more surprising to see such significant drops of CFM concentration when crossing the vertical lines (walls of abrupt changes of molecular orientation) separating various bands. Indeed, given that any possible microlensing or scattering effects can generate only a local nonmonotonic jump of the fluorescence intensity, while the fluorescence intensities observed in our work have the character of very large scale and uniform "plateau" (from both sides of defect walls), there is no doubt that we observe abruptly changing concentration levels. Indeed, the gradient of CFM concentration is increased

FIG. 6. Zoom in (a) and out (b) of one horizontal line.

at those frontiers by an order of magnitude. This shows that the molecular orientation walls are literally creating barriers for the diffusion of those molecules.

Before concluding, we also need to discuss the origins of horizontal lines (perpendicular to the contact interface) observed in our experiment [see the inset of Fig. 2(a)]. A closer look at those lines shows that they have a complex multilayer structure. Sometimes they also show intense bright fluorescence in the middle of the line [Fig. 6(a)] surrounded by low fluorescence intensity zones. That is why one possible hypothesis was that those lines might be channels of propagation of CFM (enhanced channels of diffusion). However, the slight shift of the focal plane of the microscope clearly shows [Fig. 6(b)] that the bright "channel" is moving in the lateral plane (from the center to the periphery). This means that the bright character of the fluorescent light in the narrow (horizontal) channels is generated by the microlensing effect. Indeed, the abruptly changing molecular orientation defect walls can create a significant refractive index gradient, thus forming a cylindrical microlens (see, e.g., [31], and references therein).

Let us note that the same (linear microlens) mechanism may also explain the small "spikes" of fluorescence intensity observed from both sides of the disclination walls [Fig. 3(b)].

Another possible hypothesis was based on the possibly anisotropic character of the fluorescence of CFMs that might be "stacked" in the horizontal defect lines adopting such specific orientation (perpendicular to chamber substrates) that increases the intensity observed. However, given that within the surrounding large bands the orientation of LC is planar, this should suggest that the fluorescence must be stronger when we observe the CFMs' fluorescence along the long molecular axis of LC (in an LC chamber where molecules are aligned perpendicular to substrates). To verify this hypothesis too, we have fabricated uniformly doped (by CFM) and planar aligned (strong condition) LC chambers where the glass substrates also had transparent uniform ITO electrodes under the PI-150 layer. It is well known that the application of an electric field (perpendicular to sandwich substrates) results in a voltage-dependent reorientation of LC molecules from their planar orientation (parallel to the sandwich substrates) to a perpendicular one [32] (by completely unwinding the helical structure for high voltages; see, e.g., [33], and references therein). By performing this experiment, we have observed a significant reduction of the fluorescence intensity (by a

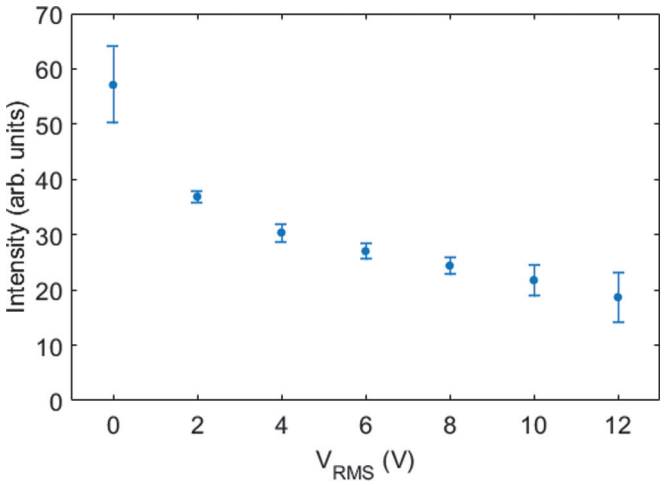

FIG. 7. Dependence of the fluorescence intensity upon the application of an electric field in the 8-μm-thick sandwich with uniformly doped CFM (in 5CB) with concentration of 0.0017 g/ml.

factor of 3) for our material system (Fig. 7). This experiment shows that the fluorescence is stronger for the observation direction that is perpendicular to the long molecular axis of LCs. Thus, compared to "uniform" bands (where the orientation of molecules is twisted and planar), the bright narrow fluorescence line (in the center of the horizontal lines) cannot be explained by the higher fluorescence due to the molecular orientation. Therefore, the cylindrical microlens effect (due to the orientation defects) remains the mechanism we use to explain the presence of intense horizontal lines. Those lines are not enhanced diffusion channels, but rather are disclination walls, while of different nature (compared to the vertical lines). This difference may be easily seen by observing the Fig. 2(a) (vertical "single" lines) and its inset (horizontal "multistructured" lines).

V. CONCLUSIONS

The diffusion of chiral molecules in liquids may be very sensitive to long-range orientational molecular interactions. This is because structural (orientation) adjustment of the host is required to allow such diffusion. Consequently, the diffusion coefficient may be noticeably reduced if the molecular system is orientationally "rigid," while still being in the liquid state. Specific abrupt molecular orientation defect walls can be naturally formed that can filter (reduce by an order of magnitude) the diffusion of chiral molecules. Those factors may be responsible for reduction of the diffusion of chiral molecules causing their aggregation. Thus, as the Brownian motion may be affected by the collective molecular reorientations [34], the diffusion of chiral molecules may be affected too and those phenomena must be taken into account in the design of chiral drugs as well as when trying to understand the propagation of chirality in the biological tissue and in nature in general [35,36]. One of the possible practical outcomes of this research might be the development of chiral filters or, in contrast, the design of specific "accompanying" molecules that would be medically passive and would have opposed twisting power (compared to the medically active molecules) to help to cross more efficiently the molecular barriers of the biological tissue.

ACKNOWLEDGMENTS

This work was made possible by a grant from the Natural Sciences and Engineering Research Council of Canada (NSERC) to T.G.

[1] L. A. Nguyen, H. He, and P.-H. Chuong, Chiral drugs: an overview, Int. J. Biomed. Sci. **2**, 85 (2006).

[2] P. Dri, Dossier Pasteur: la vie est asymétrique, Pour la Science **33**, 36 (2007).

[3] K. Peddireddy, P. Kumar, S. Thutupalli, S. Herminghaus, and C. Bahr, Myelin structures formed by thermotropic smectic liquid crystals, Langmuir **29**, 15682 (2013).

[4] C. Viney, A. E. Huber, and P. Verdugo, Liquid-crystalline order in mucus, Macromolecules **26**, 852 (1993).

[5] B. I. Kupchinov, S. F. Ermakov, V. G. Rodnenkov, S. N. Bobrysheva, E. D. Beloenko, and V. N. Kestelman, Role of liquid crystals in the lubrication of living joints, Smart Mater. Struct. **2**, 7 (1993).

[6] P. R. Secor, J. M. Sweere, L. A. Michaels, A. V. Malkovskiy, D. Lazzareschi, E. Katznelson, J. Rajadas, M. E. Birnbaum, A. Arrigoni, K. R. Braun, S. P. Evanko, D. A. Stevens, W. Kaminsky, P. K. Singh, W. C. Parks, and P. L. Bollyky, Filamentous bacteriophage promote biofilm assembly and function, Cell Host Microbe **18**, 549 (2015).

[7] A. D. Rey, E. Herrera-Valencia, and Y. K. Murugesan, Structure and dynamics of biological liquid crystals, Liq. Cryst. **41**, 430 (2014).

[8] E. Prade, C. Barucker, R. Sarkar, Gerhard Althoff-Ospelt, J. Miguel Lopez del Amo, S. Hossain, Y. Zhong, G. Multhaup, and B. Reif, Sulindac sulfide induces the formation of large oligomeric aggregates of the Alzheimer's disease amyloid-β peptide which exhibit reduced neurotoxicity, Biochemistry **55**, 1839 (2016).

[9] T. Galstian and K. Allahverdyan, Molecular self-assemblies might discriminate the diffusion of chiral molecules, Soft Matter **11**, 4167 (2015).

[10] H. Hakemi and M. M. Labes, New optical method for studying anisotropic diffusion in liquid crystals, J. Chem. Phys. **61**, 4020 (1974).

[11] H. Hakemi, A dynamic approach to study variable diffusion coefficients in nematic liquid crystals, J. Appl. Phys. **53**, 5333 (1982).

[12] S. Oehler, R. Stannarius, and H. Schmiedel, NMR investigation of the pitch dependence of self-diffusion in cholesteric liquid crystals, Z. Naturforsch., A: Phys. Sci. **43**, 687 (1988).

[13] K. K. Karukstis, E. H. Z. Thompson, J. A. Whiles, and R. J. Rosenfeld, Deciphering the fluorescence signature of daunomycin and doxorubicin, Biophys. Chem. **73**, 249 (1998).

[14] H. Zhang, T. Yu, Y. Zhao, D. Fan, L. Chen, Y. Qiu, L. Qian, K. Zhang, and C. Yang, Crystal structure and photoluminescence of 7-(*N*, *N*′-diethylamino)-coumarin-3-carboxylic acid, Spectrochim. Acta, Part A **69**, 1136 (2008).

[15] A. R. Katritzky, A. Abdelmajeid, S. R. Tala, M. S. Amine, and P. J. Steel, Novel fluorescent aminoxy acids and aminoxy hybrid peptides, Synthesis 83 (2011).

[16] T. Yu, P. Zhang, Y. Zhao, H. Zhang, J. Meng, and D. Fan, Synthesis, characterization and high-efficiency blue electroluminescence based on coumarin derivatives of 7-diethylamino-coumarin-3-carboxamide, Org. Electron. **10**, 653 (2009).

[17] T. Berthelot, J.-C. Talbot, G. Laïn, G. Déléris, and L. Latxague, Synthesis of N$^{\varepsilon}$-(7-diethylaminocoumarin-3-carboxyl)- and N$^{\varepsilon}$-(7-methoxycoumarin-3-carboxyl)-L-fmoc lysine as tools for protease cleavage detection by fluorescence, J. Peptide Sci. **11**, 153 (2005).

[18] R. H. Vekariya and H. D. Patel, Recent advances in the synthesis of coumarin derivatives via Knoevenagel condensation: A review, Synth. Commun. **44**, 2756 (2014).

[19] C. A. Lipinski, F. Lombardo, B. W. Dominy, and P. J. Feeny, Experimental and computational approaches to estimate solubility and permeability in drug discovery and development settings, Adv. Drug Delivery Rev. **46**, 3 (2001).

[20] D. F. Veber, S. R. Johnson, H.-Y. Cheng, B. R. Smith, K. W. Ward, and K. D. Kopple, Molecular properties that influence the oral bioavailability of drug candidates, J. Med. Chem. **45**, 2615 (2002).

[21] K. Palm, P. Stenberg, K. Luthman, and P. Artursson, Polar molecular surface properties predict the intestinal absorption of drugs in humans, Pharm. Res. **14**, 568 (1997).

[22] K. Takatoh, M. Hasegawa, M. Koden, N. Itoh, R. Hasegawa, and M. Sakamoto, *Alignment Technologies and Applications of Liquid Crystal Devices* (Taylor & Francis, London, 2005).

[23] P. G. de Gennes and J. Prost, *The Physics of Liquid Crystals*, 2nd ed. (Oxford University, Oxford, 1995).

[24] G. Celebre, G. De Luca, M. Maiorino, F. Iemma, A. Ferrarini, S. Pieraccini, and G. P. Spada, Solute-solvent interactions and chiral induction in liquid crystals, J. Am. Chem. Soc. **127**, 11736 (2005).

[25] I. I. Smalyukh and O. D. Lavrentovich, Three-dimensional director structures of defects in Grandjean-Cano wedges of cholesteric liquid crystals studied by fluorescence confocal polarizing microscopy, Phys. Rev. E **66**, 051703 (2002).

[26] H. de Vries, Acta Crystallogr. **4**, 219 (1951).

[27] P. P. Karat and N. V. Madhusudana, Elastic and optical properties of some 4′-*n*-alkyl-4-cyanobiphenyls, Mol. Cryst. Liq. Cryst. **36**, 51 (1976).

[28] A. D. Rey, Theory and simulation of gas diffusion in cholesteric liquid crystal films, Mol. Cryst. Liq. Cryst. **293**, 87 (1997).

[29] J. Crank, *The Mathematics of Diffusion* (Clarendon Press, Oxford University Press, Oxford, 1975).

[30] M. Pumpa and F. Cichos, Slow single-molecule diffusion in liquid crystals, J. Phys. Chem. B **116**, 14487 (2012).

[31] V. V. Presnyakov, K. E. Asatryan, T. Galstian, and A. Tork, Tunable polymer-stabilized liquid crystal microlens, Opt. Express **10**, 865 (2002).

[32] L. M. Blinov and V. G. Chigrinov, *Electrooptic Effects in Liquid Crystal Materials* (Springer, Berlin, 1996).

[33] K. Allahverdyan and T. Galstian, Electrooptic jumps in natural helicoidal photonic bandgap structures, Opt. Express **19**, 4611 (2011).

[34] Turiv, I. Lazo, A. Brodin, B. I. Lev, V. Reiffenrath, V. G. Nazarenko, and O. D. Lavrentovich, Effect of collective molecular reorientations on Brownian motion of colloids in nematic liquid crystal, Science **342**, 1351 (2013).

[35] M. Rossi, G. Zanchetta, S. Klussmann, N. A. Clark, and T. Bellini, Propagation of Chirality in Mixtures of Natural and Enantiomeric DNA Oligomers, Phys. Rev. Lett. **110**, 107801 (2013).

[36] G. Saher, B. Brugger, C. Lappe-Siefke, W. Mobius, R.-I. Tozawa, M. C. Wehr, F. Wieland, S. Ishibashi, and K.-A. Nave, High cholesterol level is essential for the myelin membrane growth, Nat. Neurosci. **8**, 468 (2005).